

# Lorentz violation and Sagnac gyroscopes

Serena Moseley,<sup>1</sup> Nicholas Scaramuzza,<sup>2</sup> Jay D. Tasson,<sup>1\*</sup> and Max L. Trostel<sup>1</sup>  
<sup>1</sup>*Physics and Astronomy Department, Carleton College, Northfield, Minnesota 55057, USA*  
<sup>2</sup>*Physics Department, St. Olaf College, Northfield, Minnesota 55057, USA*

(Dated: August 2019)

Sagnac gyroscopes with increased sensitivity are being developed and operated with a variety of goals including the measurement of General-Relativistic effects. We show that such systems can be used to search for Lorentz violation within the field-theoretic framework of the Standard-Model Extension, and that competitive sensitivities can be achieved. Special deviations from the inverse square law of gravity are among the phenomena that can be effectively sought with these systems. We present the necessary equations to obtain sensitivities to Lorentz violation in relevant experiments.

## I. INTRODUCTION

Sagnac interferometers [1] have a long history as rotation sensors and have found application in inertial guidance systems [2]. Increasingly, researchers are turning to these instruments for other applications including the measurement of geophysical effects and as a means of testing fundamental physics [3]. Some such efforts are aimed at measuring General-Relativistic phenomena including gravitomagnetic fields [4]. In General Relativity, moving masses provide additional perturbations to spacetime over sources at rest. When one considers the linearized limit of the nonlinear theory of gravity provided by General Relativity, these effects appear as a nearly direct analogue of the magnetic fields generated by moving charges in electrodynamics.

Light-based Sagnac interferometers consist of counterpropagating modes for light in a ring-shaped interferometer. The beat frequency between the modes is then observed. The non-inertial frame effects generated when the system is rotated, as well as the effect of gravitomagnetic fields can be understood as breaking the symmetry between the clockwise and counterclockwise modes, which leads to the beat signal [4]. Matter-wave Sagnac interferometers are also in use and the analogous effect on matter waves [5] is among the effects utilized by these devices to sense rotation [6].

In this work, we demonstrate that violations of Lorentz invariance described by the field-theoretic framework of the gravitational Standard-Model Extension (SME) [7, 8] can also be the source of the broken symmetry in interferometric gyroscopes and can broadly mimic rotating-frame effects in such systems. Hence sensitive interferometric gyroscopes can also be used to search for Lorentz violation in the SME [9, 10].

Lorentz invariance, the invariance of physics under rotations and boosts, lies at the foundation of our current best theories: Einstein's General Relativity and the Standard Model of particle physics. Hence testing Lorentz invariance to the best of our ability is essential. Moreover, it is widely expected that General Relativity and the Standard Model, a pair of separate theories restricted to their own domains, are merely the low-energy limit of a single more fundamental theory at the Planck scale. It has been shown that Lorentz violation may arise in

some candidates for the fundamental theory [11]. Hence a systematic search for violations of Lorentz invariance across physics may reveal hints of the underlying theory with present-day technology.

A comprehensive theoretical framework is an essential tool for a systematic search. The SME provides that framework for Lorentz-violation searches [7, 8, 12, 13]. The SME is developed at the level of the action by adding all Lorentz-violating terms to the action for known physics. These terms consist of Lorentz-violating operators constructed from the fields of General Relativity and the Standard Model coupled to coefficients (or coefficient fields) for Lorentz violation. The coefficients can then be measured or constrained by experiment and observation. The SME also provides a framework for theoretical study of Lorentz symmetry [14]

A large number of experimental and observational searches have been performed in the context of the SME [15]. This includes considerable work in the gravity sector, where experiments and observations have been done following a number of phenomenological works [14, 16–20]. Recent gravitational tests include those found in Refs. [21–25]. The tests proposed here have the potential to compete with the existing tests above and complement existing discussions of Lorentz violation in interferometric gyroscopes performed in the context of other models and frameworks [4, 9].

In the remainder of this work, we demonstrate how sensitive interferometric gyroscopes may generate additional sensitivities to gravity-sector SME coefficients. In Sec. II we review aspects of Lorentz violation in the SME relevant for the development to follow. Section III develops the form of the Lorentz-violation signal in the systems of interest. We discuss some applications of this generic result to existing experiments and those under development in Sec. IV. Throughout this paper we use natural units except where otherwise noted along with the other conventions of Ref. [16].

## II. BASIC THEORY

The SME expansion can be thought of in analogy with a series expansion. Terms are classified by the mass dimension  $d$  of the Lorentz-violating operators added to known physics [26]. The action for the Standard Model and General Relativity consists of dimension 3 and 4 operators. Hence the leading Lorentz-violating corrections to known physics are asso-

---

\* Corresponding author, jtasson@carleton.edu

ciated with operators of mass dimension 3 and 4, which form the minimal SME. Higher mass-dimension Lorentz-violating operators are also of interest as models exist which generate higher mass-dimension terms in the absence of minimal terms. In what follows we focus primarily on the gravity sector, for which the minimal and linearized nonminimal actions were developed in Refs. [8] and [18], respectively.

Post-Newtonian analyses have been performed for mass-dimension 4 and 5 Lorentz-violating operators to obtain the metric from the action in Riemann spacetime [16, 20]. In the analysis to follow, we consider only the leading contributions from Lorentz violation to a post-Newtonian expansion as the inclusion of subleading terms does not lead to additional interesting sensitivities in the relevant experiments. The following contributions to the metric were found at the Newtonian level of the post-Newtonian expansion:

$$\begin{aligned} g_{00} &= -1 + 2U + 3\bar{s}^{00}U + \bar{s}^{jk}U^{jk} \\ g_{0j} &= -\bar{s}^{0j}U - \bar{s}^{0k}U^{jk} + \frac{1}{2}\hat{Q}^j\chi \\ g_{jk} &= \delta^{jk} + (2 - \bar{s}^{00})\delta^{jk}U \\ &\quad + (\bar{s}^{lm}\delta^{jk} - \bar{s}^{jl}\delta^{mk} - \bar{s}^{kl}\delta^{jm} + 2\bar{s}^{00}\delta^{jl}\delta^{km})U^{lm}. \end{aligned} \quad (1)$$

Note that although these are Newtonian-order contributions to the metric, some will appear as post-Newtonian contributions to certain observables as they are multiplied by additional relativistic factors. Here  $U$  is the Newtonian potential,

$$U = G \int d^3x' \frac{\rho(\vec{x}', t)}{R}, \quad (2)$$

where  $G$  is Newton's constant,  $\rho$  is mass density, and  $R$  is the magnitude of  $R^j = x^j - x'^j$ , the vector pointing from the source position  $x'^j$  to the observation point  $x^j$ . It is also convenient to introduce the superpotential [16, 27]:

$$\chi = -G \int d^3x' \rho(\vec{x}', t)R, \quad (3)$$

and the additional potential

$$U^{jk} = \partial_j \partial_k \chi + \delta_{jk} U. \quad (4)$$

The object  $\bar{s}^{\mu\nu}$  is a  $d = 4$  coefficient for Lorentz violation that provides the relevant minimal gravity-sector effects. It is symmetric and traceless, hence minimal Lorentz violation in this limit is characterized by 9 components. The operator  $\hat{Q}^j$  is defined as

$$\hat{Q}^j = [q^{(5)0jkl0lm} + q^{(5)n0knljm} + q^{(5)njknl0m}] \partial_k \partial_l \partial_m, \quad (5)$$

in terms of the  $d = 5$  coefficient for Lorentz violation  $q^{(5)\mu\rho\nu\beta\sigma\gamma}$ , having symmetries defined in Ref. [18]. In the analysis to follow, the  $d = 5$  coefficients appear in the combinations

$$K_{jklm} = -\frac{1}{6}(q_{0jk0l0m}^{(5)} + q_{n0knljm}^{(5)} + q_{njknl0m}^{(5)} + \text{perms}), \quad (6)$$

where perms indicates all symmetric permutations of the indices  $klm$ . We express the 15 independent combinations of  $K_{jklm}$  that are observable in this work in terms of the canonical set introduced in Ref. [21]. The coefficients for Lorentz

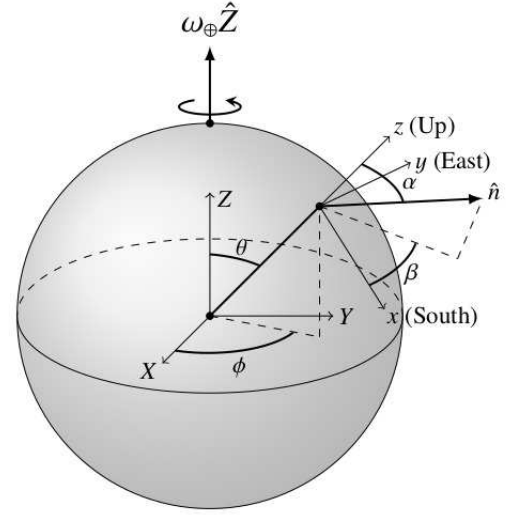


FIG. 1. Diagram showing the coordinates and angles used to describe the location and orientation of experiments in this work.

violation can be understood as characterizing the amount of Lorentz violation in the theory. In accordance with the discussion in Ref. [16], the coefficients for Lorentz violation satisfy  $\partial_\alpha \bar{s}^{\mu\nu} = 0$  and  $\partial_\delta q^{(5)\mu\rho\nu\beta\sigma\gamma} = 0$  in the asymptotically inertial Cartesian coordinates used here.

We note in passing that the techniques presented here can also, in principle, be used to probe Lorentz violation in matter-gravity couplings [17, 28]. Lorentz-violating effects associated with the source material can be incorporated in a straightforward way using the post-Newtonian metric presented in Ref. [17]. For matter-wave interferometers, the coefficients for Lorentz violation associated with the matter in the interferometer are also relevant and the associated signals have been presented elsewhere for other interferometer configurations [17]. Given the current strength of sensitivities in the matter sector, we avoid further consideration of matter-sector Lorentz violation in this work.

In the analysis to follow it is convenient to introduce three coordinate systems. A Sun-centered celestial equatorial frame with basis vectors  $\hat{Z}$  aligned with Earth's spin axis,  $\hat{X}$  pointing toward the vernal equinox in the year 2000, and  $\hat{Y}$  completing the right-handed system is the standard frame in which SME sensitivities are reported [15]. We denote the associated coordinates  $T, X, Y, Z$ . We also make use of a set of coordinates aligned with the Sun-centered coordinates and centered at the Earth denoted  $\bar{i}, \bar{x}, \bar{y}, \bar{z}$ . Finally, we introduce a laboratory basis  $\hat{x}, \hat{y}, \hat{z}$  in which  $\hat{z}$  points vertically up,  $\hat{x}$  points south, and  $\hat{y}$  completes the right-handed set. We then introduce the following angles necessary to describe the location of any Earth-based laboratory. Let  $\theta$  be the polar angle in the Earth-based coordinates corresponding to the colatitude of the experiment, and let  $\phi$  be the corresponding azimuthal angle around the Earth measured from the  $X$ -axis. These coordinates and angles are shown in Fig. 1.

When considering experiments with Earth as the source (ap-

proximated as spherical), the potentials can be written

$$U = \frac{GM_{\oplus}}{\bar{r}}, \quad (7)$$

and

$$U^{\bar{j}\bar{k}} = \frac{GM_{\oplus}\bar{r}^{\bar{j}}\bar{r}^{\bar{k}}}{\bar{r}^3} - \frac{GI_{\oplus}}{3\bar{r}^5}[3\bar{r}^{\bar{j}}\bar{r}^{\bar{k}} - \delta^{\bar{j}\bar{k}}\bar{r}^2], \quad (8)$$

where  $M_{\oplus}$  is the mass of the Earth,  $\bar{r}^{\bar{j}}$  are components of a position vector in the Earth-centered frame, and  $\bar{r}$  is the magnitude of position. The quantity

$$I_{\oplus} = \int d^3\bar{r}' \rho(\bar{r}') \bar{r}'^2 \quad (9)$$

is the spherical moment of inertia of the Earth. For later convenience we define the scaled spherical moment,

$$i_{\oplus} = \frac{I_{\oplus}}{M_{\oplus}R_{\oplus}^2}, \quad (10)$$

which has a value of approximately 0.50 [29], as well as the symbol

$$i_n = 1 + ni_{\oplus}. \quad (11)$$

Here  $R_{\oplus}$  is the radius of the Earth and  $n$  is a real number.

### III. GYROSCOPE ANALYSIS

In this section, we review the aspects of interferometric gyroscope measurements of spacetime properties that are relevant for our analysis of Lorentz violation before applying these tools to the general theory of Lorentz violation above.

#### A. Spacetime probe

##### 1. Light

We begin in analogy with a metric-based approach to the analysis of rotating-frame and gravitomagnetic effects in photon-based systems [4]. Lightlike trajectories satisfy the null condition

$$0 = g_{\mu\nu} dx^{\mu} dx^{\nu}. \quad (12)$$

When  $g_{0j}$  is nonzero in the proper frame of the experiment, 2 solutions for the time taken for a photon to travel around a loop emerge from the null condition for a suitably chosen loop. The difference in these times is the difference in the time taken to go around the loop in opposite directions. Considering measurements made in a laboratory at rest with coordinates  $x_L^j$  in a stationary metric, the proper time difference measured in this frame can be written

$$\Delta\tau = 2 \sqrt{g_{00}(x_L^j)} \oint \frac{g_{0j}}{g_{00}} dx^j. \quad (13)$$

However in the analysis to follow, we consider the leading effects involving the first power of coefficients for Lorentz violation. Higher powers of Lorentz violation as well as Lorentz violation suppressed by post-Newtonian effects beyond the Newtonian level or noninertial frame effects associated with the rotation of an Earth-based laboratory are significantly smaller relative to the leading effects of Lorentz violation, and they are not considered. Further, we do not present the standard Lorentz-invariant contributions to the interferometric-gyroscope signal as these have been well studied elsewhere [4]. With these specializations and the metric (1), it suffices to write

$$\Delta\tau \approx 2 \oint g_{0j} dx^j. \quad (14)$$

Continuing at leading order, the phase difference in the counterpropagating modes per orbit is

$$\Delta\psi = 2\pi \frac{\Delta\tau}{\lambda}, \quad (15)$$

where  $\lambda$  is the wavelength of the light. Hence the number of orbits per beat cycle is

$$N = \frac{\lambda}{\Delta\tau}. \quad (16)$$

The beat period can be written as

$$T = NP, \quad (17)$$

where  $P$  is the perimeter of the loop. Thus the beat frequency is

$$f_b = \frac{\Delta\tau}{\lambda P}. \quad (18)$$

For the cases of interest here, the integral in Eq. (14) is most straightforwardly evaluated by analogy with Ampere's law, with  $g_{0j}$  playing the role of the magnetic field. The curl of  $g_{0j}$  then plays the role of the current density, which we call  $2\vec{\Omega}$  due to its relation to the angular velocity of the lab in the context of Sagnac experiments. Denoting with  $\vec{\Omega}^{(s)}$  the rotating frame contribution to  $\vec{\Omega}$ , one finds, for example,

$$\vec{\Omega}^{(s)} = \vec{\omega}_{\oplus} \quad (19)$$

for a device at rest on the Earth, where  $\vec{\omega}_{\oplus}$  is Earth's angular velocity. For other contributions to  $g_{0j}$ ,  $\vec{\Omega}$  can be understood as an effective rotation rate, an analogy that is useful in estimating sensitivities to fundamental-physics effects.

Continuing by analogy with Ampere's law,  $\Delta\tau$  can be written as the integral over the area enclosed by the loop as follows

$$\Delta\tau = 4 \int \vec{\Omega} \cdot \hat{n} dA, \quad (20)$$

where  $\hat{n}$  is a unit vector normal to the loop. To evaluate  $\Delta\tau$  it is convenient to introduce several angles. Let  $\alpha$  be a polar angle in the laboratory measured from the laboratory  $z$ -axis to  $\hat{n}$ ,

and let  $\beta$  be an azimuthal angle around the laboratory vertical from the laboratory  $x$ -axis to  $\hat{n}$ . Figure 1 shows these definitions. For the cases of interest, the area of the interferometer is sufficiently small that  $\vec{\Omega}$  can be taken as uniform over its extent and the integral in Eq. (20) can be evaluated as a simple product.

## 2. Matter waves

Though we consider light-based Sagnac gyroscopes in detail above, the notion of  $\vec{\Omega}$  as an effective rotation rate typically applies to matter-wave Sagnac gyroscopes as well. In atom-interferometer gyroscopes, an atom beam is typically split and recombined using light pulses in such a way that the beam paths enclose an area [30]. In these systems, the phase difference of the beams at recombination provides the signal.

In the context of Sagnac-like signals at leading order in  $\vec{\Omega}$ , there are 2 relevant mechanisms by which the phase is impacted: the phase accumulated during free propagation between light pulses and the effect of the light pulses [5]. The free propagation contribution can be calculated by integrating the Lagrangian around the loop. This calculation is completely analogous to that done for photons above, and it leads to a phase difference of the form of Eq. (15) with the wavelength given by the Compton wavelength of the interfering particles of mass  $m$ :

$$\lambda \rightarrow \frac{1}{m}, \quad (21)$$

and  $\Delta\tau$  given by Eq. (20). This result is sometimes conveniently expressed [6] in terms of the total time the particle spends in the interferometer  $T$ , the effective wave vector of the pulses  $\vec{k}$ , and the initial momentum of the atoms  $\vec{p}$ , in which case it is proportional to  $\frac{1}{m}(\vec{\Omega} \times \vec{k}) \cdot \vec{p}T^2$ .

The phase imprint due to the light pulses depends on the locations at which the light-atom interactions occur. Since  $\vec{\Omega}$  alters the path of the atoms through the equation of motion, a signal also arises here. For a particle in an Earth-based laboratory, the relevant parts of the equation of motion are

$$\vec{a} = \vec{g} - 2\vec{\Omega} \times \vec{v}, \quad (22)$$

where  $\vec{v}$  is the velocity of the atoms and  $\vec{g}$  is the local gravitational field. Applying the solutions to this equation to atom interferometers [6] yields a leading phase shift proportional to  $\vec{k} \cdot (\vec{g} \times \vec{\Omega})T^3$ . Though typically smaller than the free-propagation signal, the interaction signal offers other advantages and is sometimes used as the dominant rotation-sensing effect.

## B. Lorentz violation

In this subsection, we apply the general gyroscope results above to Lorentz violation in the SME. We first consider the minimal SME, and then higher mass-dimension terms.

### 1. The minimal SME

The leading minimal Lorentz-violating effects on gyroscopes are described by the 3 degrees of freedom contained in  $\vec{s}^{TJ}$ . Due to its relative simplicity, we apply the above results to the minimal SME first. To obtain the dominant  $\vec{s}^{\mu\nu}$  effects on the beat frequency of laboratory gyroscopes, it suffices to apply the above methods with the metric (1) expressed in Earth-centered coordinates in a spherical-Earth approximation, where we find that the dominant Lorentz-violating contributions to  $\vec{\Omega}$  at  $d = 4$  can be written

$$\vec{\Omega}^{(4)} = \vec{s} \times \vec{g}, \quad (23)$$

where  $\vec{s} = \vec{s}^{\vec{j}}$ . Transforming the metric to laboratory coordinates would yield the usual Sagnac term along with Lorentz-violating corrections to it. Such suppressed corrections take us beyond Newtonian order hence they are not considered here. The Earth-centered components  $\vec{s}^{ij}$  are equal to the Sun-centered frame components  $\vec{s}^{TJ}$  up to terms suppressed by the boost of the Earth on its orbit around the Sun, a suppression factor of  $10^{-4}$ .

Note that  $\vec{\Omega}^{(4)}$ , which is proportional to the effective current density in the Ampere's law analogy, has no radial component. Hence laser-gyroscope loops having  $\hat{n}$  radial, will involve no leading Lorentz-violation signal from  $\vec{s}^{TJ}$ . The explicit form of the polar and azimuthal components in Earth-centered spherical coordinates offers some additional insights into the structure of the signal:

$$\Omega_\theta^{(4)} = \frac{GM_\oplus}{R_\oplus^2} (\vec{s}^{\vec{i}\vec{x}} \sin \phi - \vec{s}^{\vec{i}\vec{y}} \cos \phi) \quad (24)$$

$$\Omega_\phi^{(4)} = \frac{GM_\oplus}{R_\oplus^2} [\cos \theta (\vec{s}^{\vec{i}\vec{x}} \cos \phi + \vec{s}^{\vec{i}\vec{y}} \sin \phi) - \vec{s}^{\vec{i}\vec{z}} \sin \theta]. \quad (25)$$

The  $\phi$  dependence of the signal in a loop oriented with  $\hat{n}$  in the polar direction is  $90^\circ$  out of phase with that of a loop oriented with  $\hat{n}$  in the azimuthal direction, and the latter orientation is the only one with sensitivity to the  $Z$  component of  $\vec{s}^{TJ}$ .

Applying the procedure outlined above, we find

$$f_b^{(4)} = \frac{4AGM_\oplus}{\lambda PR_\oplus^2} \sin \alpha \left[ \cos \beta (\vec{s}^{\vec{i}\vec{x}} \sin \phi - \vec{s}^{\vec{i}\vec{y}} \cos \phi) + \sin \beta (\cos \theta (\vec{s}^{\vec{i}\vec{x}} \cos \phi + \vec{s}^{\vec{i}\vec{y}} \sin \phi) - \vec{s}^{\vec{i}\vec{z}} \sin \theta) \right] \quad (26)$$

for the explicit form of the leading  $d = 4$  contributions to the beat frequency in a laser-gyroscope system of arbitrary orientation described by the angles  $\alpha$  and  $\beta$  and arbitrary Earth-based location specified by the angles  $\theta$  and  $\phi$ .

In the context of matter-wave interferometers, we also present the explicit form of the potentially useful combination  $\vec{k} \cdot (\vec{g} \times \vec{\Omega}^{(4)})$ . To do so, we write  $\vec{k}$  in laboratory polar coordinates again using  $\alpha$  and  $\beta$  as the laboratory polar and azimuthal angles respectively, and take  $\vec{g}$  as radial:

$$\vec{k} \cdot (\vec{g} \times \vec{\Omega}^{(4)}) = \frac{kG^2M_\oplus^2}{R_\oplus^4} \sin \alpha \left[ \sin \beta (\vec{s}^{\vec{i}\vec{y}} \cos \phi - \vec{s}^{\vec{i}\vec{x}} \sin \phi) + \cos \beta (\cos \theta (\vec{s}^{\vec{i}\vec{x}} \cos \phi + \vec{s}^{\vec{i}\vec{y}} \sin \phi) - \vec{s}^{\vec{i}\vec{z}} \sin \theta) \right].$$

Coeff.	$\Omega_r^{(5)}$	$\Omega_\theta^{(5)}$	$\Omega_\phi^{(5)}$
$K_{XXXY}$	$-12(3i_{-5/3}c3\theta + 5i_{-3/5}c\theta - 12i_{-5/3}c2\phi c\theta s^2\theta)$	$-3(6i_{-5}c^2\phi s3\theta + 7i_{-3/7}s\theta + 15i_{1/3}c2\phi s\theta)$	$36i_{-5/3}s2\phi s2\theta$
$K_{XXXZ}$	$12s\theta(5i_{-3/5}s\phi + 3i_{-5/3}s\phi c2\theta - 6i_{-5/3}s3\phi s^2\theta)$	$3s\phi(11i_{-7/11} - 3i_{-5}c2\theta)c\theta + 9i_{-5}s3\phi s2\theta s\theta$	$3(-7i_{-3/7}c\phi + 15i_{1/3}c\phi c2\theta + 6i_{-5}c3\phi s^2\theta)$
$K_{XXYY}$	$144i_{-5/3}s2\phi c\theta s^2\theta$	$-18s2\phi(3i_{-5/9} + i_{-5}c2\theta)s\theta$	$-36i_{-5/3}c2\phi s2\theta$
$K_{XXYZ}$	$-12(-3i_{-5/3}c\phi s3\theta + i_1c\phi s\theta - 12i_{-5/3}c3\phi s^3\theta)$	$6c\theta(-5i_{7/5}c\phi - 3i_{-5}c\phi c2\theta - 6i_{-5}c3\phi s^2\theta)$	$-6(i_3s\phi - 9i_{-5/9}s\phi c2\theta - 6i_{-5}s3\phi s^2\theta)$
$K_{XXZZ}$	$-144i_{-5/3}s2\phi c\theta s^2\theta$	$-18s2\phi(i_{5/3} - i_{-5}c2\theta)s\theta$	$-12(3 + 5i_{\oplus}c2\phi)s2\theta$
$K_{XYYY}$	$-4(3i_{-5/3}c3\theta + 5i_{-3/5}c\theta + 12i_{-5/3}c2\phi c\theta s^2\theta)$	$-6i_{-5}s^2\phi s3\theta - 7i_{-3/7}s\theta + 15i_{1/3}c2\phi s\theta$	$-12i_{-5/3}s2\phi s2\theta$
$K_{XYYZ}$	$12s\theta(7i_{-9/7}s\phi + 9i_{-5/3}s\phi c2\theta + 6i_{-5/3}s3\phi s^2\theta)$	$3c\theta(s\phi(i_{-21} - 9i_{-5}c2\theta) - 6i_{-5}s3\phi s^2\theta)$	$-3(5i_{-9/5}c\phi + 3i_{-5}c\phi c2\theta + 6i_{-5}c3\phi s^2\theta)$
$K_{XYYZ}$	$12(3i_{-5/3}c3\theta + i_{-3}c\theta + 12i_{-5/3}c2\phi c\theta s^2\theta)$	$-3(-6i_{-5}s^2\phi s3\theta + i_3s\theta - 9i_{-5/9}c2\phi s\theta)$	$-60i_{\oplus}s2\phi s2\theta$
$K_{XZZZ}$	$-16s\phi(i_{-3} + 3i_{-5/3}c2\theta)s\theta$	$-4s\phi(7i_{-1} - 3i_{-5}c2\theta)c\theta$	$-4c\phi(i_3 + 3i_{5/3}c2\theta)$
$K_{YXXZ}$	$12s\theta(-7i_{-9/7}c\phi - 9i_{-5/3}c\phi c2\theta + 6i_{-5/3}c3\phi s^2\theta)$	$-3c\theta(c\phi(i_{-21} - 9i_{-5}c2\theta) + 6i_{-5}c3\phi s^2\theta)$	$3(-5i_{-9/5}s\phi - 3i_{-5}s\phi c2\theta + 6i_{-5}s3\phi s^2\theta)$
$K_{YXYZ}$	$-24s\theta(i_{-3}s\phi + 3i_{-5/3}s\phi c2\theta - 6i_{-5/3}s3\phi s^2\theta)$	$6s\phi c\theta(5i_{7/5} + 3i_{-5}c2\theta) - 18i_{-5}s3\phi s2\theta s\theta$	$-6(i_3c\phi - 9i_{-5/9}c\phi c2\theta + 6i_{-5}c3\phi s^2\theta)$
$K_{YXZZ}$	$-12(3i_{-5/3}c3\theta + i_{-3}c\theta - 12i_{-5/3}c2\phi c\theta s^2\theta)$	$-3(6i_{-5}c^2\phi s3\theta - i_3s\theta - 9i_{-5/9}c2\phi s\theta)$	$-60i_{\oplus}s2\phi s2\theta$
$K_{YYYZ}$	$-12s\theta(5i_{-3/5}c\phi + 3i_{-5/3}c\phi c2\theta + 6i_{-5/3}c3\phi s^2\theta)$	$-3c\theta(11i_{-7/11}c\phi - 3i_{-5}c\phi c2\theta - 6i_{-5}c3\phi s^2\theta)$	$-3(7i_{-3/7}s\phi - 15i_{1/3}s\phi c2\theta + 6i_{-5}s3\phi s^2\theta)$
$K_{YZZZ}$	$144i_{-5/3}s2\phi c\theta s^2\theta$	$6s2\phi(3i_{5/3} - 3i_{-5}c2\theta)s\theta$	$12(-3 + 5i_{\oplus}c2\phi)s2\theta$
$K_{YZZZ}$	$16c\phi(i_{-3} + 3i_{-5/3}c2\theta)s\theta$	$4c\phi(7i_{-1} - 3i_{-5}c2\theta)c\theta$	$-4s\phi(i_3 + 3i_{5/3}c2\theta)$

TABLE I. The components of the quantity  $\vec{\Omega}^{(5)}$  in spherical coordinates are constructed by multiplying the expressions in each row under a given component with the corresponding coefficient for Lorentz violation appearing in the first column, summing over all rows, then multiplying the sum by the overall factor,  $\frac{GM_\oplus}{32K_\oplus}$ . For example,  $\Omega_r^{(5)} = \frac{GM_\oplus}{32K_\oplus}(-12(3i_{-5/3}c3\theta + 5i_{-3/5}c\theta - 12i_{-5/3}c2\phi c\theta s^2\theta)K_{XXXY} + 12s\theta(5i_{-3/5}s\phi + 3i_{-5/3}s\phi c2\theta - 6i_{-5/3}s3\phi s^2\theta)K_{XXXZ} + \dots)$ . For brevity, trig functions are abbreviated with their first letter ( $s = \sin, c = \cos$ ).

Coeff.	$A_1$	$A_2$	$A_3$
$K_{XXXY}$	0	$36i_{-5/3}s\alpha s\beta s2\theta$	0
$K_{XXXZ}$	$3sac\beta c\theta(11i_{-7/11} - 3i_{-5}c2\theta) + 12c\alpha s\theta(5i_{-3/5} + 3i_{-5/3}c2\theta)$	0	$18s^2\theta(i_{-5}sac\beta c\theta - 4i_{-5/3}c\alpha s\theta)$
$K_{XXYY}$	0	$18s\theta(8i_{-5/3}c\alpha c\theta s\theta - sac\beta(3i_{-5/9} + i_{-5}c2\theta))$	0
$K_{XXYZ}$	$-6s\alpha s\beta(i_3 - 9i_{-5/9}c2\theta)$	0	$36i_{-5}s\alpha s\beta s^2\theta$
$K_{XXZZ}$	0	$-18s\theta(8i_{-5/3}c\alpha c\theta s\theta + sac\beta(i_{5/3} - i_{-5}c2\theta))$	0
$K_{XYYY}$	0	$-12i_{-5/3}s\alpha s\beta s2\theta$	0
$K_{XYYZ}$	$3sac\beta c\theta(i_{-21} - 9i_{-5}c2\theta) + 12c\alpha s\theta(7i_{-9/7} + 9i_{-5/3}c2\theta)$	0	$18s^2\theta(4i_{-5/3}c\alpha s\theta - i_{-5}sac\beta c\theta)$
$K_{XYYZ}$	0	$-60i_{\oplus}s\alpha s\beta s2\theta$	0
$K_{XZZZ}$	$-4sac\beta c\theta(7i_{-1} - 3i_{-5}c2\theta) - 16c\alpha s\theta(i_{-3} + 3i_{-5/3}c2\theta)$	0	0
$K_{YXXZ}$	$-3s\alpha s\beta(5i_{-9/5} + 3i_{-5}c2\theta)$	0	$18i_{-5}s\alpha s\beta s^2\theta$
$K_{YXYZ}$	$6sac\beta c\theta(5i_{7/5} + 3i_{-5}c2\theta) + 12c\alpha(-3i_{-5/3}s3\theta + i_1s\theta)$	0	$36s^2\theta(4i_{-5/3}c\alpha s\theta - i_{-5}sac\beta c\theta)$
$K_{YXZZ}$	0	$-60i_{\oplus}s\alpha s\beta s2\theta$	0
$K_{YYYZ}$	$3s\alpha s\beta(-7i_{-3/7} + 15i_{1/3}c2\theta)$	0	$-18i_{-5}s\alpha s\beta s^2\theta$
$K_{YZZZ}$	0	$6s\theta(sac\beta(3i_{5/3} - 3i_{-5}c2\theta) + 24i_{-5/3}c\alpha c\theta s\theta)$	0
$K_{YZZZ}$	$-4s\alpha s\beta(i_3 + 3i_{5/3}c2\theta)$	0	0

TABLE II. Amplitudes of  $\sin n\phi$  harmonics of the beat frequency appearing in Eq. (28). For brevity, trig functions are abbreviated with their first letter ( $s = \sin, c = \cos$ ). The explicit form of each amplitude  $A_n$  is constructed by multiplying the expressions in each row under the amplitude  $A_n$  with the corresponding coefficient for Lorentz violation appearing in the first column and summing over all rows.

(27)

## 2. Mass-dimension 5 signals

It should be noted that Lorentz-violating contributions to an effective  $\vec{g}$  in the lab could, in principle, be of interest and can arise at leading order in Lorentz violation when multiplied by Lorentz-invariant contributions to  $\vec{\Omega}$ . In the context of our present focus on  $\vec{s}^{TJ}$  and  $K_{JKLM}$  these contributions are suppressed relative to those that arise from Eq. (27).

The signals generated by Lorentz-violating operators of higher mass dimension in gyroscope systems can be generated by following the same procedures used at  $d = 4$  provided that the metric is available. With the metric contributions at  $d = 5$  now available [21] as presented in Eq. (1), we present the associated signals in interferometric gyroscope experiments.

The results are most neatly expressed by characterizing the 15 Lorentz-violating degrees of freedom appearing in the  $d = 5$  signal in terms of the 15 canonical  $K_{jklm}$  coefficients

Coeff.	$B_1$	$B_2$	$B_3$
$K_{XXXX}$	0	$72 i_{-5/3} c \alpha s 2 \theta s \theta - 18 s a c \beta s \theta (3 i_{-5/9} + i_{-5} c 2 \theta)$	0
$K_{XXXZ}$	$3 s \alpha s \beta (-7 i_{-3/7} + 15 i_{1/3} c 2 \theta)$	0	$18 i_{-5} s \alpha s \beta s^2 \theta$
$K_{XXYY}$	0	$-36 i_{-5/3} s \alpha s \beta s 2 \theta$	0
$K_{XXYZ}$	$-6 s a c \beta c \theta (5 i_{7/5} + 3 i_{-5} c 2 \theta) + 24 c \alpha s \theta (i_{-3} + 3 i_{-5/3} c 2 \theta)$	0	$36 s^2 \theta (4 i_{-5/3} c \alpha s \theta - i_{-5} s a c \beta c \theta)$
$K_{XXZZ}$	0	$-60 i_{\oplus} s \alpha s \beta s 2 \theta$	0
$K_{XYYY}$	0	$6 s \theta (s a c \beta (3 i_{-5/9} + i_{-5} c 2 \theta) - 4 i_{-5/3} c \alpha s 2 \theta)$	0
$K_{XYYZ}$	$-3 s \alpha s \beta (5 i_{-9/5} + 3 i_{-5} c 2 \theta)$	0	$-18 i_{-5} s \alpha s \beta s^2 \theta$
$K_{XYZZ}$	0	$18 s \theta (s a c \beta (i_{5/3} - i_{-5} c 2 \theta) + 4 i_{-5/3} c \alpha s 2 \theta)$	0
$K_{XZZZ}$	$-4 s \alpha s \beta (i_3 + 3 i_{5/3} c 2 \theta)$	0	0
$K_{YXXZ}$	$-3 s a c \beta c \theta (i_{-21} - 9 i_{-5} c 2 \theta) - 12 c \alpha s \theta (7 i_{-9/7} + 9 i_{-5/3} c 2 \theta)$	0	$18 s^2 \theta (4 i_{-5/3} c \alpha s \theta - i_{-5} s a c \beta c \theta)$
$K_{YXYZ}$	$-6 s \alpha s \beta (i_3 - 9 i_{-5/9} c 2 \theta)$	0	$-36 i_{-5} s \alpha s \beta s^2 \theta$
$K_{YXZZ}$	0	$18 s \theta (s a c \beta (i_{5/3} - i_{-5} c 2 \theta) + 4 i_{-5/3} c \alpha s 2 \theta)$	0
$K_{YYYZ}$	$3 s a c \beta c \theta (3 i_{-5} c 2 \theta - 11 i_{-7/11}) - 6 c \alpha (3 i_{-5/3} s 3 \theta + 7 i_{-1/7} s \theta)$	0	$18 s^2 \theta (i_{-5} s a c \beta c \theta - 4 i_{-5/3} c \alpha s \theta)$
$K_{YYZZ}$	0	$60 i_{\oplus} s \alpha s \beta s 2 \theta$	0
$K_{YZZZ}$	$4 s a c \beta c \theta (7 i_{-1} - 3 i_{-5} c 2 \theta) + 16 c \alpha s \theta (i_{-3} + 3 i_{-5/3} c 2 \theta)$	0	0

TABLE III. Amplitudes  $B_n$  of  $\cos n\phi$  harmonics of the beat frequency appearing in (28) constructed as in Table II.

Coeff.	$A_0$
$K_{XXXX}$	$-12 s a c \beta s \theta (4 i_{-3} c^2 \theta + i_3 s^2 \theta) - 48 c a c \theta (2 i_{-1} c^2 \theta - i_{-3} s^2 \theta)$
$K_{XXXZ}$	$-36 s \alpha s \beta s 2 \theta$
$K_{XXYY}$	$-4 s a c \beta s \theta (4 i_{-3} c^2 \theta + i_3 s^2 \theta) - 16 c a c \theta (2 i_{-1} c^2 \theta - i_{-3} s^2 \theta)$
$K_{XYYZ}$	$24 (2 i_{-2} c a c^3 \theta + i_{-6} s a c \beta c^2 \theta s \theta)$
$K_{XYZZ}$	$-12 (4 i_{-3/2} c \alpha s 2 \theta s \theta + i_{-3} s a c \beta s^3 \theta)$
$K_{YXXZ}$	$24 (2 i_{-2} c a c^3 \theta + i_{-6} s a c \beta c^2 \theta s \theta)$
$K_{YXZZ}$	$-12 (4 i_{-3/2} c \alpha s 2 \theta s \theta + i_{-3} s a c \beta s^3 \theta)$
$K_{YZZZ}$	$-36 s \alpha s \beta s 2 \theta$

TABLE IV. The time-independent contributions to the beat frequency appearing in (28) constructed as in Table II.

introduced in Ref. [21]. While the form of the signal at  $d = 5$  provides some experimental advantages, the associated expressions are more lengthy. The content of  $\vec{\Omega}^{(5)}$ , the  $d = 5$  contributions to  $\vec{\Omega}$ , is presented in Table I.

To present the key results in a way that efficiently highlights trends, we decompose the expressions by harmonics of the angle  $\phi$ , and hence harmonics of the sidereal frequency. The beat frequency in a laser-gyroscope system can be written

$$f_b^{(5)} = \frac{AGM_{\oplus}}{8\lambda PR_{\oplus}^3} \left( A_0 + \sum_{n=1}^3 (A_n \sin n\phi + B_n \cos n\phi) \right). \quad (28)$$

The amplitudes  $A_n$  and  $B_n$  containing the coefficients for Lorentz violation and the remaining angles describing the location and orientation of the ring are presented in Tables II - IV. Entries in the tables take the form of experiment-specific numbers, again highlighting the feature that measurements performed with different orientations and in different Earth-based locations will measure different linear combinations of coefficients for Lorentz violation. Note that the signal at  $d = 5$  involves up to the 3rd harmonic of  $\phi$ .

Proceeding to provide the analogous information in the  $d =$

5 case, the combination  $\vec{k} \cdot (\vec{g} \times \vec{\Omega}^{(5)})$  takes the form

$$\vec{k} \cdot (\vec{g} \times \vec{\Omega}^{(5)}) = \frac{kG^2 M_{\oplus}^2}{32R_{\oplus}^5} \left( C_0 + \sum_{n=1}^3 (C_n \sin n\phi + D_n \cos n\phi) \right), \quad (29)$$

where the amplitudes  $C_n, D_n$  are provided in Tables V and VI using the same structure as in the case of  $f_b^{(5)}$ .

#### IV. EXPERIMENTS AND MEASUREMENTS

In this section we offer some additional comments on translating experimental results into measurements of the canonical forms of the coefficients for Lorentz violation. We also discuss the sensitivities that existing devices and those in development are likely to achieve.

In the present context of Earth-based experiments,  $\phi = \omega_{\oplus} t + \phi_0$ . Here  $\omega_{\oplus}$  is the Earth's sidereal angular frequency,  $t$  is the local sidereal time, and  $\phi_0$  is a phase induced by the fact that  $\phi$  as defined in this work is not, in general, zero at the zero of local sidereal time. This will be true only for experiments performed at the longitude for which the Sun was directly overhead at the equator at the moment of the vernal equinox in the year 2000. Based on data from the United States Naval Observatory [31], this longitude  $l_0 \approx 66.25^\circ$ . For experiments at other longitudes  $l$  in degrees, this makes [32]

$$\phi_0 = \frac{2\pi}{360} (l_0 - l). \quad (30)$$

While Eqs. (26) and (28) can be fit to data from any laser-gyroscope system, we point out a few features that may help identify a Lorentz-violation signal among other signal and noise sources. With the exception of special orientations, the Lorentz-violation signal contains both constant effects and effects periodic at the sidereal frequency and its harmonics. Such periodicity is not expected for the other signals with

Coeff.	$C_0$	$C_1$	$C_2$	$C_3$
$K_{XXXY}$	$6s\alpha s\beta s\theta(5i_{-9/5} + 3i_{-5}c2\theta)$	0	$36i_{-5/3}s\alpha c\beta s2\theta$	0
$K_{XXXZ}$	0	$3s\alpha s\beta c\theta(-11i_{-7/11} + 3i_{-5}c2\theta)$	0	$-9i_{-5}s\alpha s\beta s2\theta s\theta$
$K_{XXYY}$	0	0	$18s\alpha s\beta s\theta(3i_{-5/9} + i_{-5}c2\theta)$	0
$K_{XXYZ}$	0	$-6s\alpha c\beta(i_3 - 9i_{-5/9}c2\theta)$	0	$36i_{-5}s\alpha c\beta s^2\theta$
$K_{XZZZ}$	$-72s\alpha c\beta c\theta s\theta$	0	$18s\alpha s\beta s\theta(i_{5/3} - i_{-5}c2\theta)$	0
$K_{XYYY}$	$2s\alpha s\beta s\theta(5i_{-9/5} + 3i_{-5}c2\theta)$	0	$-12i_{-5/3}s\alpha c\beta s2\theta$	0
$K_{XYYZ}$	0	$3s\alpha s\beta c\theta(-i_{-21} + 9i_{-5}c2\theta)$	0	$9i_{-5}s\alpha s\beta s2\theta s\theta$
$K_{XYYZ}$	$-6s\alpha s\beta s\theta(i_9 + 3i_{-5}c2\theta)$	0	$-60i_{\oplus}s\alpha c\beta s2\theta$	0
$K_{XZZZ}$	0	$-4s\alpha s\beta c\theta(-7i_{-1} + 3i_{-5}c2\theta)$	0	0
$K_{YXXZ}$	0	$-3s\alpha c\beta(5i_{-9/5} + 3i_{-5}c2\theta)$	0	$18i_{-5}s\alpha c\beta s^2\theta$
$K_{YXYZ}$	0	$-6s\alpha s\beta c\theta(5i_{7/5} + 3i_{-5}c2\theta)$	0	$36i_{-5}s\alpha s\beta c\theta s^2\theta$
$K_{YXZZ}$	$6s\alpha s\beta s\theta(i_9 + 3i_{-5}c2\theta)$	0	$-60i_{\oplus}s\alpha c\beta s2\theta$	0
$K_{YYYZ}$	0	$3s\alpha c\beta(-7i_{-3/7} + 15i_{1/3}c2\theta)$	0	$-18i_{-5}s\alpha c\beta s^2\theta$
$K_{YZZZ}$	$-72s\alpha c\beta c\theta s\theta$	0	$18s\alpha s\beta s\theta(-i_{5/3} + i_{-5}c2\theta)$	0
$K_{YZZZ}$	0	$-4s\alpha c\beta(i_3 + 3i_{5/3}c2\theta)$	0	0

TABLE V. Amplitudes  $C_n$  of  $\sin n\phi$  harmonics of the matter-wave factor appearing in Eq. (29), constructed as in Table II.

Coeff.	$D_1$	$D_2$	$D_3$
$K_{XXXY}$	0	$18s\alpha s\beta s\theta(3i_{-5/9} + i_{-5}c2\theta)$	0
$K_{XXXZ}$	$3s\alpha c\beta(-7i_{-3/7} + 15i_{1/3}c2\theta)$	0	$18i_{-5}s\alpha c\beta s^2\theta$
$K_{XXYY}$	0	$-36i_{-5/3}s\alpha c\beta s2\theta$	0
$K_{XXYZ}$	$6s\alpha s\beta c\theta(5i_{7/5} + 3i_{-5}c2\theta)$	0	$36i_{-5}s\alpha s\beta c\theta s^2\theta$
$K_{XZZZ}$	0	$-60i_{\oplus}s\alpha c\beta s2\theta$	0
$K_{XYYY}$	0	$-6s\alpha s\beta s\theta(3i_{-5/9} + i_{-5}c2\theta)$	0
$K_{XYYZ}$	$-3s\alpha c\beta(5i_{-9/5} + 3i_{-5}c2\theta)$	0	$-18i_{-5}s\alpha c\beta s^2\theta$
$K_{XYYZ}$	0	$18s\alpha s\beta s\theta(-i_{5/3} + i_{-5}c2\theta)$	0
$K_{XZZZ}$	$-4s\alpha c\beta(i_3 + 3i_{5/3}c2\theta)$	0	0
$K_{YXXZ}$	$-3s\alpha s\beta c\theta(-i_{-21} + 9i_{-5}c2\theta)$	0	$9i_{-5}s\alpha s\beta s2\theta s\theta$
$K_{YXYZ}$	$-6s\alpha c\beta(i_3 - 9i_{-5/9}c2\theta)$	0	$-36i_{-5}s\alpha c\beta s^2\theta$
$K_{YXZZ}$	0	$18s\alpha s\beta s\theta(-i_{5/3} + i_{-5}c2\theta)$	0
$K_{YYYZ}$	$-3s\alpha s\beta c\theta(-11i_{-7/11} + 3i_{-5}c2\theta)$	0	$-9i_{-5}s\alpha s\beta s2\theta s\theta$
$K_{YZZZ}$	0	$60i_{\oplus}s\alpha c\beta s2\theta$	0
$K_{YZZZ}$	$4s\alpha s\beta c\theta(-7i_{-1} + 3i_{-5}c2\theta)$	0	0

TABLE VI. Amplitudes  $D_n$  of  $\cos n\phi$  harmonics of the matter-wave factor appearing in Eq. (29), constructed as in Table II.

perhaps the exception of tidal disturbances. Moreover, the conventional effects such as the dominant kinematic effect of the rotating frame of the earth and gravitomagnetic effects do not generate signals for systems in which  $\hat{n}$  is along  $\hat{\phi}$  making the existence and form of a signal in a system so oriented potentially of significant use. In addition to these special features, like the signals from conventional General-Relativistic effects, the Lorentz-violation signal can be distinguished from the dominant kinematic effect via comparison with sensitive earth-rotation measurements from sources such as Very Long Baseline Interferometry.

The aim of devices under development is to measure general relativistic effects that appear in these experiments analogous to a rotation of order  $10^{-9}\omega_{\oplus}$ , and sensitivity near this level has already been achieved [3]. Hence devices under development aim to exceed this level of sensitivity [3, 33]. Given the form of the effective rotation rate in Eq. (23), sensitivities

to the  $\vec{s}^{IJ}$  coefficients can be crudely estimated using SI units as follows:

$$\vec{s}^{IJ} \approx \frac{\epsilon\omega_{\oplus}cR_{\oplus}^2}{GM_{\oplus}}. \quad (31)$$

Here  $\epsilon$  is the fractional sensitivity to  $\omega_{\oplus}$  and  $c$  is the speed of light. With  $\epsilon \approx 10^{-9}$ , Eq. (31) yields an estimated sensitivity to Lorentz violation of order  $10^{-6}$ . This suggests advanced interferometric gyroscope experiments are likely to be competitive with other laboratory [25, 34] and perhaps Solar-System experiments [24] measuring  $\vec{s}^{IJ}$ . Though they are unlikely to compete with constraints set by astrophysical observations [23, 35], laboratory tests are often thought of differently due to the enhanced control and understanding available to experiments over observations.

Though the specifics vary among the  $d = 5$  coefficients, the dominant feature that appears when comparing with the

estimated sensitivity to the minimal coefficients is the additional factor of distance to the source in the beat frequency (28). This can also be seen from the form of  $\vec{\Omega}^{(5)}$  presented in Table I, where the coefficients for Lorentz violation enter  $\vec{\Omega}^{(5)}$  multiplied by  $\frac{GM_{\oplus}}{R_{\oplus}^3}$  along with a numerical factor of up to order 1. Hence the  $d = 5$  sensitivities can be crudely estimated as

$$K_{JKLM} \approx \frac{\epsilon\omega_{\oplus}cR_{\oplus}^3}{GM_{\oplus}}, \quad (32)$$

which suggests  $d = 5$  sensitivities better than 10 m are possible. Sensitivities at this level would be competitive with the best existing measurements of these coefficients, which currently come from binary-pulsar analysis [21].

The capabilities of laser-gyroscope systems relative to other kinds of tests can be understood from a combination of features. First, Lorentz violation entering the metric in  $g_{0j}$  is

typically suppressed in post-Newtonian tests by the relative speed of the source and test bodies. In light-based gyroscopes, this issue is obviated by the use of light to probe the metric. In comparison with the pulsar tests, Earth-based gyroscope experiments amount to a shorter-range test, which offers a relative advantage at  $d = 5$ , an advantage that could be expected to grow with mass dimension. In fact, interferometric gyroscopes may offer a novel system in which to search for short-range velocity-dependent forces, a qualitatively new type of signal in the search for new physics.

## ACKNOWLEDGMENTS

The authors gratefully acknowledge the following for financial support: S.M. from the Carleton College Summer Science Fellows Program and N.S. from the St. Olaf College CURI fund. We also acknowledge useful conversations with D. Atkinson, Q. Bailey, A. Di Virgilio, and M. Seifert.

- 
- [1] G. Sagnac, C.R. Acad. Sci. **157**, 708 (1913).  
[2] A. Lawrence, *Modern Inertial Technology*, (Springer, New York, 1998).  
[3] See, for example, N. Beverini, A. D. Virgilio, J. Belfi, A. Ortolan, K. U. Schreiber, A. Gebauer, and T. Klügel, J. Phys. Conf. Ser. **723**, 012061 (2016).  
[4] F. Bosi, G. Cella, A. Di Virgilio, A. Ortolan, A. Porzio, S. Solimeno, M. Cerdonio, J. P. Zendri, M. Allegrini, J. Belfi, *et al.*, Phys. Rev. D **84**, 122002 (2011).  
[5] P. Storey and C. Cohen-Tannoudji, J. Phys. II **4**, 1999 (1994).  
[6] B. Dubetsky and M. A. Kasevich, Phys. Rev. A **74**, 023615 (2006).  
[7] D. Colladay and V. A. Kostelecký, Phys. Rev. D **58**, 116002 (1998), arXiv:hep-ph/9809521 [hep-ph].  
[8] V. A. Kostelecký, Phys. Rev. D **69**, 105009 (2004), arXiv:hep-th/0312310 [hep-th].  
[9] For earlier discussion of the basic idea, see, M. L. Ruggiero, Galaxies **3**, 84 (2015), arXiv:1505.01268 [gr-qc].  
[10] For earlier discussion of a special case, see, N. Scaramuzza and J. D. Tasson, in *CPT and Lorentz Symmetry VII*, edited by V. Kostelecký (2017) pp. 271–273, arXiv:1607.08111 [gr-qc].  
[11] V. A. Kostelecký and S. Samuel, Phys. Rev. D **39**, 683 (1989); V. A. Kostelecký and R. Potting, Nucl. Phys. B **359**, 545 (1991).  
[12] For a review, see J. D. Tasson, Rep. Prog. Phys. **77**, 062901 (2014), arXiv:1403.7785 [hep-ph].  
[13] For a pedagogical introduction to Lorentz violation, see, T. H. Bertshinger, N. A. Flowers, S. Moseley, C. R. Pfeifer, J. D. Tasson, and S. Yang, Symmetry **11**, 22 (2019).  
[14] Q. G. Bailey and C. D. Lane, Symmetry **10**, 480 (2018), arXiv:1810.05136 [hep-th]; V. A. Kostelecký and Z. Li, Phys. Rev. D **99**, 056016 (2019), arXiv:1812.11672 [hep-ph]; B. R. Edwards and V. A. Kostelecký, Phys. Lett. B **786**, 319 (2018), arXiv:1809.05535 [hep-th]; V. A. Kostelecký and A. J. Vargas, Phys. Rev. D **92**, 056002 (2015), arXiv:1506.01706 [hep-ph]; V. A. Kostelecký and R. Lehnert, *ibid.* **63**, 065008 (2001), arXiv:hep-th/0012060 [hep-th]; Y. Bonder and C. Corral, Symmetry **10**, 433 (2018), arXiv:1808.05522 [gr-qc]; M. Seifert, *ibid.* **10**, 490 (2018); R. Bluhm and A. Schic, Phys. Rev. D **94**, 104034 (2016), arXiv:1610.02892 [hep-th].  
[15] V. A. Kostelecký and N. Russell, *Data tables for Lorentz and CPT violation*, 2018 Edition, arXiv:0801.0287v12 [hep-ph].  
[16] Q. G. Bailey and V. A. Kostelecký, Phys. Rev. D **74**, 045001 (2006), arXiv:gr-qc/0603030 [gr-qc].  
[17] V. A. Kostelecký and J. D. Tasson, Phys. Rev. D **83**, 016013 (2011), arXiv:1006.4106 [gr-qc].  
[18] V. A. Kostelecký and M. Mewes, Phys. Lett. B **757**, 510 (2016).  
[19] V. A. Kostelecký and M. Mewes, Phys. Lett. B **766**, 137 (2017), arXiv:1611.10313 [gr-qc]; **779**, 136 (2018), arXiv:1712.10268 [gr-qc]; Q. G. Bailey, A. Kostelecký, and R. Xu, Phys. Rev. D **91**, 022006 (2015), arXiv:1410.6162 [gr-qc]; M. Mewes, **99**, 104062 (2019), arXiv:1905.00409 [gr-qc].  
[20] Q. G. Bailey and D. Havert, Phys. Rev. D **96**, 064035 (2017).  
[21] L. Shao and Q. G. Bailey, Phys. Rev. D **98**, 084049 (2018).  
[22] L. Shao and Q. G. Bailey, Phys. Rev. D **99**, 084017 (2019), arXiv:1903.11760 [gr-qc].  
[23] C.-G. Shao, Y.-F. Chen, Y.-J. Tan, S.-Q. Yang, J. Luo, M. E. Tobar, J. C. Long, E. Weisman, and V. A. Kostelecký, Phys. Rev. Lett. **122**, 011102 (2019); B. P. Abbott *et al.* (LIGO Scientific, Virgo, Fermi-GBM, and INTEGRAL Collaborations), Astrophys. J. **848**, L13 (2017), arXiv:1710.05834 [astro-ph.HE]; C.-G. Shao, Y.-F. Chen, R. Sun, L.-S. Cao, M.-K. Zhou, Z.-K. Hu, C. Yu, and H. Müller, Phys. Rev. D **97**, 024019 (2018), arXiv:1707.02318 [gr-qc].  
[24] A. Bourgoin, C. Le Poncin-Lafitte, A. Hees, S. Bouquillon, G. Francou, and M.-C. Angonin, Phys. Rev. Lett. **119**, 201102 (2017), arXiv:1706.06294 [gr-qc].  
[25] N. A. Flowers, C. Goodge, and J. D. Tasson, Phys. Rev. Lett. **119**, 201101 (2017), arXiv:1612.08495 [gr-qc].  
[26] For a pedagogical discussion of mass dimension in the SME, see, J. D. Tasson, JPS Conf. Proc. **18**, 011002 (2017), arXiv:1708.03213 [hep-ph].  
[27] C. M. Will, *Theory and experiment in gravitational physics* (Cambridge, University Press, Cambridge, England, 1993).  
[28] V. A. Kostelecký and J. Tasson, Phys. Rev. Lett. **102**, 010402 (2009), arXiv:0810.1459 [gr-qc].  
[29] W. Shen, Z. Yang, Z. Guo, and W. Zhang, Geod. Geodyn. **10**, 118 (2019).



- [30] F. Riehle, T. Kisters, A. Witte, J. Helmcke, and C. J. Bordé, *Phys. Rev. Lett.* **67**, 177 (1991); T. L. Gustavson, P. Bouyer, and M. A. Kasevich, **78**, 2046 (1997); J. K. Stockton, K. Takase, and M. A. Kasevich, **107**, 133001 (2011); D. Savoie, M. Alto-rio, B. Fang, L. A. Sidorenkov, R. Geiger, and A. Landragin, *Sci. Adv.* **4**, eaau7948 (2018).
- [31] United States Naval Observatory, web-site, <https://aa.usno.navy.mil/data/docs/EarthSeasons.php>, Accessed: May 2, 2019.
- [32] Y. Ding and V. A. Kostelecký, *Phys. Rev. D* **94**, 056008 (2016), arXiv:1608.07868 [hep-ph].
- [33] A. D. V. Di Virgilio, J. Belfi, W.-T. Ni, N. Beverini, G. Carelli, E. Maccioni, and A. Porzio, *Eur. Phys. J. Plus* **132**, 157 (2017).
- [34] K.-Y. Chung, S.-W. Chiow, S. Herrmann, S. Chu, and H. Muller, *Phys. Rev. D* **80**, 016002 (2009), arXiv:0905.1929 [gr-qc]; H. Muller, S.-w. Chiow, S. Herrmann, S. Chu, and K.-Y. Chung, *Phys. Rev. Lett.* **100**, 031101 (2008), arXiv:0710.3768 [gr-qc].
- [35] V. A. Kostelecký and J. D. Tasson, *Phys. Lett. B* **749**, 551 (2015), arXiv:1508.07007 [gr-qc].